Journal of Hazardous Materials, 7 (1983) 291—302
Elsevier Scientific Publishing Company, Amsterdam — Printed in The Netherlands

UTILIZATION OF ACCELERATING RATE CALORIMETRY FOR THE CHARACTERIZATION OF ENERGETIC MATERIALS AT MRC-MOUND

J. M. PICKARD
MRC-Mound*, Miamisburg, Ohio 45342

ABSTRACT

The technique of Accelerating Rate Calorimetry (ARC) was used to investigate the thermal stabilities of energetic materials used in production and manufacturing at MRC-Mound. Plots of heat rate versus temperature, along with temperature and pressure versus time plots, were determined for selected secondary explosives and one model compound. Analyses of these data were used to derive zero-order kinetic parameters, time-to-explosion plots, and approximate critical explosion temperatures.

INTRODUCTION

Because of potential hazards associated with storage and processing of explosives and energetic compounds, techniques to assess the thermal stabilities and explosion potential of reactive compounds are of considerable interest. In the past, techniques such as differential scanning calorimetry (DSC) and differential thermal analysis (DTA) were the primary methods used in hazard analysis (ref. 1). However, these techniques fail to address possible pressure hazards, which, in some instances, could pose more serious problems than those associated with thermal explosions. The limitations of DSC and DTA are overcome with a new technique involving accelerating rate calorimetry (refs. 2-4).

As part of a program to assess potential safety hazards, ARC measurements were initiated to characterize energetic compounds routinely used in production and manufacturing at MRC-Mound. In this paper, the theory of ARC operation is reviewed, and preliminary results are presented on the characterization of selected secondary explosives and one model compound.

*MRC-Mound is operated by Monsanto Research Corporation for the U. S. Department of Energy under Contract No. DE-AC04-76-DP00053.

EXPERIMENTAL

All explosives examined in this work consisted of production grade materials and were used without further purification. Samples consisted of the following: pentaerythritol tetranitrate (PETN), hexanitroazobenzene (HNAB), 2-(5-cyanotetrazolato) pentaammine cobalt(III) perchlorate (CP), 1,3,5-trinitro-s-triazine (RDX), PBX-9407, and the model compound 5-cyanotetrazole (5-CNTZ).

Adiabatic calorimetric measurements were obtained with a commercial accelerating rate calorimeter manufactured and distributed by Columbia Scientific Industries Corp. The operation of the ARC has been described in detail elsewhere (refs. 4-5). Briefly, it involves monitoring the heat rate, temperature and pressure change of an exothermic reaction under adiabatic conditions. The sample is enclosed in a spherical bomb, which, in turn, is connected to a pressure transducer and thermocouple. Adiabatic conditions are maintained by three cartridge heaters located at the top, side, and bottom of a cylindrical jacket surrounding the sample bomb. During an exothermic reaction, temperature differences between the bomb and three zones of the jacket are maintained at zero by standard differential, integral, and control algorithms.

All measurements were conducted in lightweight stainless steel bombs under an air atmosphere. In a typical ARC run, the sample was heated to an initial temperature of 30°C. After equilibration at 30°C, an iterative "5°C heat-30 min wait-search" sequence was conducted until the appearance of a heat rate greater than 0.02°C/min. After detection of the exotherm, heat rate, pressure, and temperature were monitored continuously until the end of the reaction. At the conclusion of each run, all relevant data were plotted automatically by the ARC microprocessor.

THEORY OF ADIABATIC CALORIMETRY

In an exothermic reaction, a quasi-stationary temperature distribution exists whenever the heat evolution and heat transfer rates are equal. If the heat evolution rate exceeds the heat transfer rate, the temperature will increase exponentially and accelerate the reaction. Figure 1 illustrates the accelerating rate and exponential temperature rise for an exothermic reaction occurring under adiabatic conditions. As shown in Fig. 1, the initial heat rate, M_0, rises to a maximum, M_m, and then decreases to zero at the final temperature, T_f. The time at temperature T required for the reaction to reach the maximum rate is designated by θ.

Figure 2 is a plot of the heat transfer and heat evolution rates versus temperature. The critical explosion temperature, T_c, is defined as the temperature at which the heat transfer rate is tangential to the heat evolution rate. Whenever $T>T_c$, the heat evolution rate will spiral upward and the system will approach conditions favorable for thermal explosion.

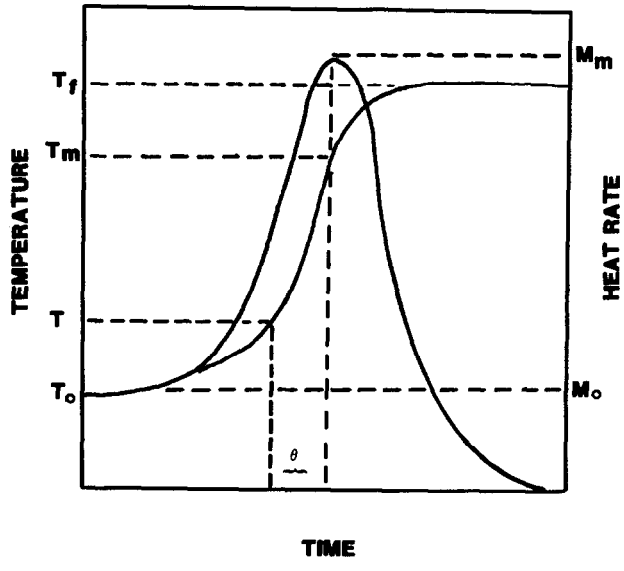

Fig. 1. Hypothetical temperature vs. time plot for an adiabatic reaction.

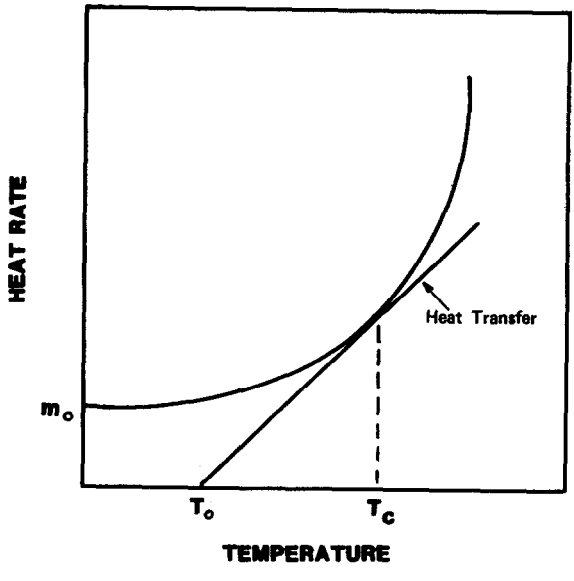

Fig. 2. Heat rate vs. temperature plot for an adiabatic reaction.

Fundamental heat rate expression

The rate of a homogeneous reaction is expressed as

$$\frac{-dX}{dt} = AT^{\alpha} e^{-E/RT} F(X) \tag{1}$$

where X is concentration, A is the preexponential factor, E is the activation energy, R is the ideal gas constant, and F(X) is a concentration function defined by the reaction mechanism. The exponent α has values of 0.0, 0.5, and 1.0 for the Arrhenius, hard sphere collision, and absolute rate theories, respectively.

In adiabatic calorimetry (refs. 4-5), F(X) is defined explicitly from temperature as

$$F(X) = X^n = \left(\frac{T_f - T}{\Delta T}\right)^n X_0^n \tag{2}$$

where n is the reaction order, X_0 is the initial concentration, and ΔT is the adiabatic temperature rise, $T_f - T_0$. Differentiation of Eq. (2) with respect to T followed by substitution into Eq. (1), assuming $\alpha = 0.0$, yields

$$M_T = \frac{dT}{dt} = Ae^{-E/RT} \left(\frac{T_f - T}{\Delta T}\right)^n \Delta T X_0^{n-1} \tag{3}$$

Equation (3) is the fundamental heat rate expression required for interpretation of ARC data. In the initial stages of reaction where $T \backsimeq T_0$ and $X \backsimeq X_0$, Eq. (3) may be simplified to

$$M_0 = \frac{dT}{dt} = Ae^{-E/RT} \Delta T X_0^{n-1} \tag{4}$$

Equation (4) is designated as the zero-order line and may be used to evaluate the Arrhenius parameters from the initial stages of the heat rate versus temperature curve generated by the ARC microprocessor.

Time to explosion, θ

The heat evolution rate in a closed system is expressed as

$$NC_v \frac{dT}{dt} = V\Delta H AT^{\alpha} e^{-E/RT} F(X) \tag{5}$$

where N is the number of moles of reactant, C_v is the molar heat capacity, V is the system volume, and ΔH is the reaction enthalpy. Since the effect of temperature upon the preexponential, AT^{α}, is rather small, Eq. (5) may be reduced to an easily integrable form by assuming $\alpha = 2$ without seriously affecting the data analysis. On this basis, Townsend (ref. 4), has shown that integration of Eq. (5) yields

$$\Theta = \frac{RT^2}{M_T E} - \frac{RT_m^2}{M_m E} \tag{6}$$

as an approximate analytical expression for the time to explosion or maximum rate. Since M_m is significantly larger than M_T, Eq. (6) simplifies to

$$\Theta \sim \frac{RT^2}{M_T E} \tag{7}$$

which is equivalent to the expression obtained for first-order decomposition of homogeneous explosives (refs. 6,7). By substituting Eq. (3) into Eq. (7) and recognizing that $\ln A >> RT^2/\left[X_0^{n-1}\left[(T_f-T)/\Delta T\right]^n \Delta TE\right]$, it follows that

$$\ln \Theta \sim \frac{E}{R}\left(\frac{1}{T}\right) - \ln A \tag{8}$$

Equation (8) provides an alternative basis for the evaluation of zero-order kinetic parameters.

Critical explosion temperature, T_c

The equilibrium that exists from equality of the heat evolution and heat transfer rates is expressed analytically as

$$NC_v\frac{dT}{dt} = V\Delta HAe^{-E/RT}F(X) = Sh(T-T_0) \tag{9}$$

where S and h are the surface area and heat transfer coefficient of the reaction vessel, respectively. Differentiation of Eq. (9) with respect to T and evaluation at T_c yields

$$NC_v\left(\frac{dT}{dt}\right)\frac{E}{RT_c^2} = Sh \tag{10}$$

By combining Eqs. (7) and (10), one obtains

$$\Theta_c = \frac{NC_v}{Sh} \tag{11}$$

where Θ_c is the adiabatic zero-order time to maximum rate at the critical temperature, T_c. For a specific reaction vessel, T_c may be determined graphically from the ARC time to maximum rate curve using Θ_c estimated from Eq. (11).

As an alternative approach (ref. 8), the critical explosion temperature may be estimated as follows. By defining a reduced temperature as $T_r = (T_c-T_0)/T_0$, Eqs. (10) and (11) may be combined to obtain

$$\frac{RT_0(T_r+1)^2}{E} = T_r = \frac{T_c-T_0}{T_0} \tag{12}$$

For a typical decomposition reaction with E~50 kcal/mol, the roots of Eq. (12) will lie within the range, $T_0 < T_r < 50T_0$; however, only the lower root will be physically significant. This implies that $T_c \sim T_0$ or that $T_r << 1$; therefore, Eq. (12) may be simplified and rearranged to yield

$$T_c \sim T_0 + \frac{RT_0^2}{E} \tag{13}$$

Equation (13) may be used to estimate T_c from the initial temperature at the onset of the exotherm and the zero-order activation energy determined from the initial portion of the heat rate versus temperature plot.

Correction for thermal inertia, ϕ

Equations discussed in the preceding sections are based on the assumption of perfect adiabaticity. However, in actual ARC experiments, part of the heat is expended by heating the sample bomb. The adiabatic temperature rise of the pure compound and the temperature increase of the system, ΔT_s, are related by

$$\Delta T = \left(1 + \frac{M_b C_{vb}}{M_s C_{vb}}\right) \Delta T_s = \phi \Delta T \tag{14}$$

where M is mass, and the subscripts s and b refer to the sample and bomb, respectively. In the initial stages of reaction, the effect of thermal inertia is to decrease the magnitude of M_0 and Θ by a constant factor. Accordingly, the fundamental and approximate relations derived from Eqs. (2) and (3) may be corrected with Eq. (14) to conditions expected for a pure compound.

RESULTS AND DISCUSSION

Figures 3 and 4 illustrate the pressure and temperature versus time plots obtained from the thermal decomposition of PETN and the inorganic explosive, CP. Both Figs. 3 and 4 are qualitatively the same, except for time scale, in the sense that the pressure rise closely approximates the exponential temperature change that accompanies exothermic decomposition under adiabatic conditions. This effect was observed for all organic explosives examined and suggests that no appreciable pressure hazard exists prior to the temperature at which significant self-heating occurs.

Plots of the self-heat rate versus the reciprocal of absolute temperature for PETN, 5-CNTZ, HNAB, and CP are given in Figs. 5-8, respectively. Zero-order lines, calculated from the temperature-time data, are indicated by the straight lines tangent to the initial portion of each of the heat rate curves. Figures 5 and 6 for PETN and 5-CNTZ both exhibit the expected rate acceleration to the maximum, which then decreases as the result of reactant depletion. The heat

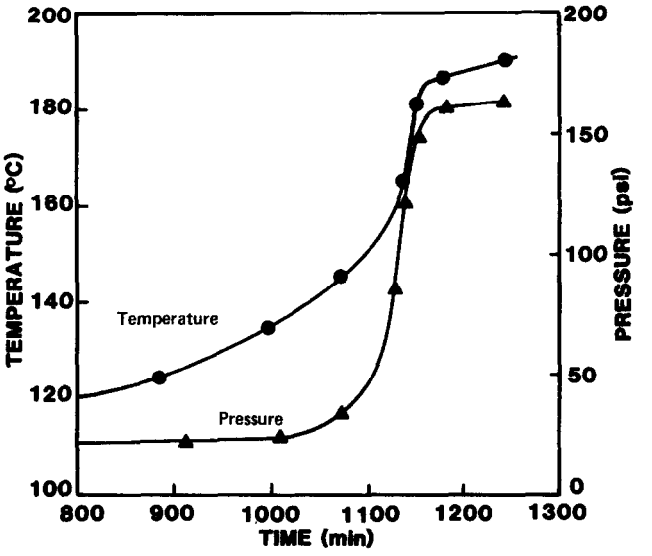

Fig. 3. Temperature and pressure vs. time plots for PETN.

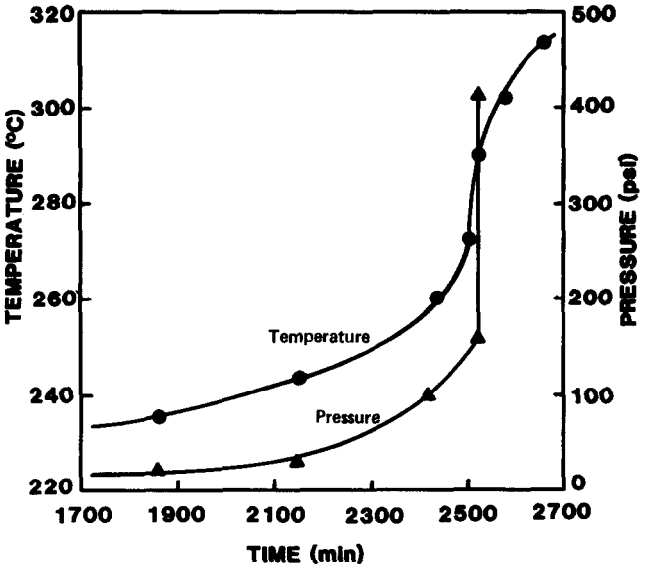

Fig. 4. Temperature and pressure vs. time plots for CP.

rate curve for PETN is representative of organic compounds that melt before appreciable decomposition occurs, while that observed for 5-CNTZ is considerably broader due to solid-state decomposition that occurs at ∿30°C below the observed melting point. The heat rate plot for HNAB fails to show the expected behavior,

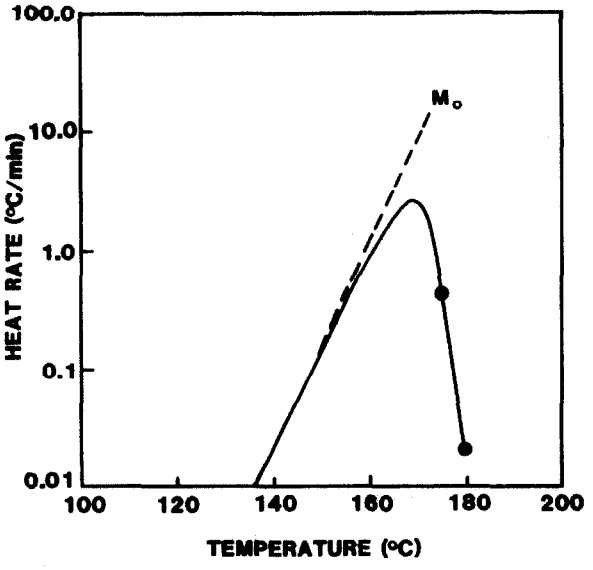

Fig. 5. Heat rate vs. temperature plot for PETN: scale 1/T, K^{-1}.

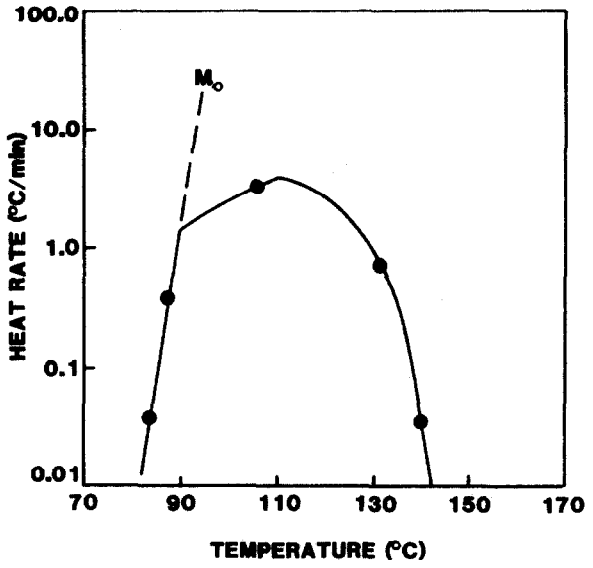

Fig. 6. Heat rate vs. temperature plot for 5-CNTZ: scale 1/T, K^{-1}.

since this particular run resulted in an actual explosion and destruction of the sample bomb. Figure 8 for CP exhibits a regular increase in rate, followed by rapid acceleration at ∿260°C. This phenomenon was not unexpected and is similar to the thermal reactivity curves obtained from DSC analysis (ref. 9).

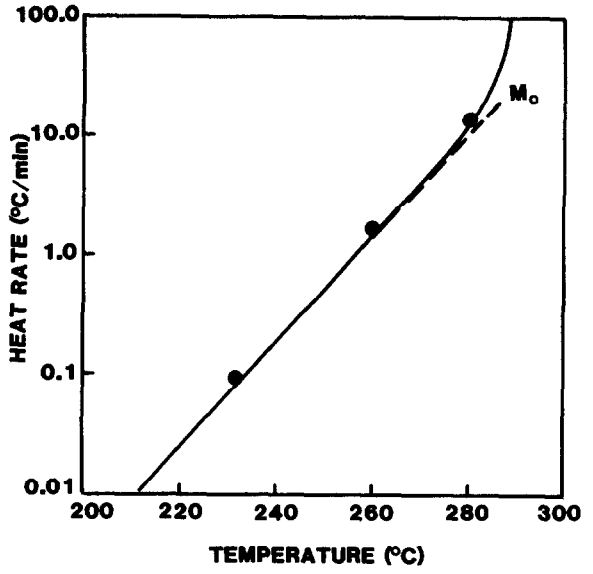

Fig. 7. Heat rate vs. temperature plot for HNAB: scale 1/T, K^{-1}.

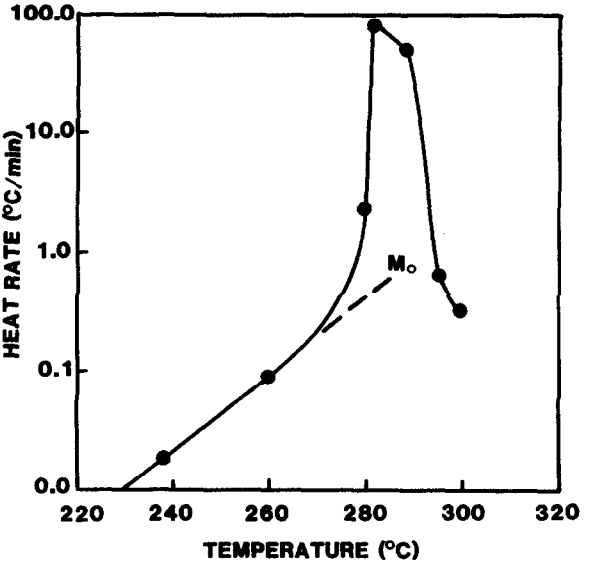

Fig. 8. Heat rate vs. temperature plot for CP: scale 1/T, K^{-1}.

Zero-order kinetic parameters

The initial heat rate versus temperature curves were corrected for thermal inertia and the resultant data were plotted according to Eq. (4). Representative rate plots with slope E/R are illustrated in Fig. 9. A summary of the kinetic

parameters evaluated from the slopes and intercepts of the plots in Fig. 9 assuming a first-order reaction are given in Table 1. DSC kinetic parameters (indicated in brackets), melting points, and the corrected onset temperatures for each exotherm are also included in Table 1 for comparison. Examination of the onset temperatures reveals that all of the explosives decompose below their reported melting points. The observed Arrhenius parameters, excluding those obtained for CP and possibly PETN, are substantially higher than the corresponding values obtained from DSC analysis. These results indicate that the decomposition mechanisms are complex and suggest that the kinetics are probably not amenable to the simple formalism of the Arrhenius theory.

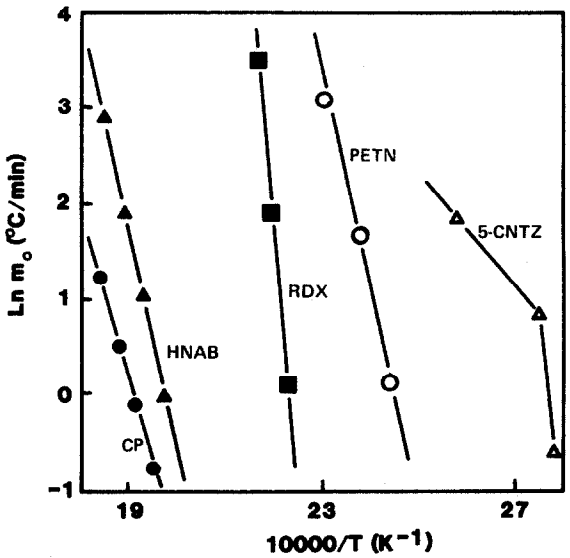

Fig. 9. Zero-order rate plot for energetic compounds.

TABLE 1

Summary of Arrhenius parameters

Compound	E^a (Kcal/mol)	$\ln A^{a,b}$ s-1	$T_0(\phi=1)$ (°C)	Melting Point (°C)	Ref.
HNAB	51.9	-	194	215	
CP	37.6 [37.0]	25.2 [35.3]	188	-	9
PETN	54.5 [47.0]	54.4 [45.6]	112	143	10
5-CNTZ	87.4 [37.0]	70.1 [40.5]	74	∿110	11
RDX	173 [47.1]	177 [42.1]	180	204	10
PBX-9407	187	201	175	200 (dec)	

[a] Bracketed entries are DSC results from Refs. 9-11.

[b] Calculated from the assumption of n=1.

Zero-order time to explosion or maximum rate

Figure 10 illustrates the time to maximum rate plots corrected for the effect of thermal inertia for HNAB, CP, RDX, PETN, and 5-CNTZ. Plots for HNAB, CP, RDX, and PETN were extrapolated, as shown by the dotted lines, on the basis of Eq. (8) from the corrected onset temperatures given in Table 1 into the temperature range normally encountered in the storage and processing of high explosives. Plots such as shown in Fig. 10 may be used to assess potential explosion hazards in temperature regions not normally amenable to experiment, provided that the mechanisms are the same in the lower temperature regions.

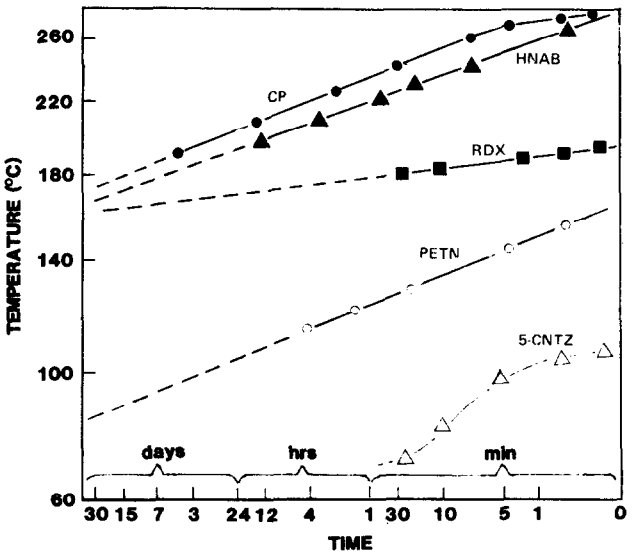

Fig. 10. Time to maximum rate plot for energetic compounds.

Critical explosion temperatures

In the storage and processing of explosives and energetic materials, the critical explosion temperature is an important parameter that is related to the available time for corrective action once an exothermic reaction has begun. In the present work, values of T_c for each compound were estimated from the observed onset temperature of each exotherm corrected for thermal inertia and the zero-order activation energy using Eq. (13). Results are summarized in Table 2 along with the corrected onset temperatures observed for each exotherm.

It is interesting to note that in Table 2, all values for T_c lie within the range of ∿2-11°C above the initial temperature at the onset of each exotherm. These data represent extrapolations (ϕ = 1) expected for pure materials, and all of the temperatures excluding those for 5-CNTZ and PETN are substantially higher than 100°C. At MRC-Mound, production operations involve the drying of neat

TABLE 2

Summary of critical explosion temperatures

Compound	T_o (°C)	T_c (°C)
HNAB	194	202
CP	188	199
PETN	112	117
5-CNTZ	74	77
RDX	180	182
PBX-9407	175	177

explosives and explosive blends under an air atmosphere in the temperature range of 60-100°C. Since the initial and critical temperatures are both considerably higher than 100°C, potential safety hazards associated with self-heating effects would not be anticipated.

SUMMARY AND CONCLUSIONS

The theory of ARC operation and its application for the characterization of explosive compounds were discussed. Preliminary ARC data for selected explosives were used to evaluate zero-order kinetic parameters and critical explosion temperatures. The observed activation energies for RDX, PBX-9407, and 5-CNTZ were substantially higher than reported DSC values. Examination of the heat rate versus temperature data revealed that all of the organic compounds exhibited solid-state decomposition. It is suggested that the simple formalism of the Arrhenius theory is probably not applicable to the decomposition of RDX and PBX-9407. Estimated critical explosion temperatures of all compounds examined suggest that thermal explosions hazards do not pose a serious problem to production operations currently conducted at MRC-Mound.

REFERENCES

1 A.A. Duswalt, Thermochemica Acta, 8(1974)57.
2 L. Walker, in Proc. 5th Int. Conf. on Chemical Thermodynamics, Ronneby, Sweden, August 1977.
3 D. I. Townsend, Chem. Eng. Prog., 73(1977)80.
4 D. I. Townsend, Thermochemica Acta, 37(1980)1.
5 CSI-ARC Manual, Columbia Scientific Industries, Austin, TX.
6 O. M. Todes, Acta Physiochim. USSR, 5(1936)75.
7 S. H. Lin and H. Eyring, Ann. Rev. Phys. Chem., 21(1970)255.
8 S. W. Benson, The Foundations of Chemical Kinetics, McGraw-Hill, New York, 1960, p. 433.
9 T. M. Massis, P. K. Morenus, D. H. Huskisson, and R. M. Merrill, in Proc. Joint Symp. on Compatibility of Plastics/Materials with Explosives and Processing Explosives, Blackburg, Virginia, October 14-16, 1980, p. 105.
10 T. R. Gibbs and P. Popolato (Eds.), LASL Explosive Property Data, University of California Press, Berkeley, California, 1980, p. 219.
11 J. M. Pickard, MRC-Mound, Miamisburg, OH, unpublished data.